Optics Communications 419 (2018) 97–102

Contents lists available at ScienceDirect

Optics Communications

journal homepage: www.elsevier.com/locate/optcom

Generation of a localized hollow laser beam using crossed nonlinear optical crystals

Zhizhang Wang [a], Chunxi Wang [a], Chunying Pei [a], Yaling Yin [a], Yong Xia [a,b,*], Jianping Yin [a]

[a] State Key Laboratory of Precise Spectroscopy, School of Physics and Materials Science, East China Normal University, Shanghai 200062, People's Republic of China
[b] Collaborative Innovation Center of Extreme Optics, Shanxi University, Taiyuan, Shanxi 030006, People's Republic of China

ARTICLE INFO

Keywords:
Localized hollow beam
Nonlinear crystal
Propagating property

ABSTRACT

A nonlinear optical approach to generate a localized hollow laser beam and its array using crossed nonlinear ZnSe crystals is proposed. We calculate the intensity distributions of the hollow beam and its propagating properties in free space, and study the dependences of the dark spot size of the hollow beam on the incident beam waist radius and the crystal length. Our studies show that the longitudinal size of the hollow beam can be reduced by ∼660 times than that generated by a single nonlinear crystal. Such laser beam with a dark hollow region and a large intensity gradient can be used to trap cold neutral atoms, molecules and microscopic particles.

1. Introduction

A localized hollow laser beam (LHB) is a kind of laser beam consisting of a dark central region that is fully surrounded by regions of high intensity [1]. Since the LHB has a three-dimension (3D) closed dark hollow region and a large intensity gradient, it can be used to trap microscopic particles and neutral atoms. So, the LHB has many important and extensive applications in modern optics and atomic (or molecular) optics [2–6]. In particular, the intensity gradient near the focal point of a LHB may be used to efficiently cool neutral atoms by LHB-induced Sisyphus cooling [7].

LHBs have been generated by a number of approaches, e.g. holograms [8], conical refraction [9–12], uniaxial crystal [13], interferometer [14], photon sieve [15], optical fiber [16], polarized light [17], focusing multi-ring hollow Gaussian beam [18], to form a desirable hollow axial structure. The concept of a LHB has also been recently extended to plasmonic structures [19,20], the plasmonic bottle beam could be used to optically sort particles by trapping those with a specific size. Nowadays, nonlinear optical methods have been proposed to generate non-diffraction beams [21–23]. Many self-action effects have been thoroughly investigated, including self-phase modulation [24], self-focusing [25–27] and self-bending [28–30]. Our approach is motivated by the self-bending (SB) effect of ZnSe nonlinear material. ZnSe is a kind of materials with large nonlinear refractive index, and it can induce the SB effect for the incident laser beam, which can be transformed to the hollow beam distribution at the optimal position by the nonlinear medium.

In this paper, we propose a scheme – using crossed ZnSe nonlinear crystals – to generate a LHB and its array, and validate this scheme theoretically. The intensity distributions of the LHB in different cases of the symmetric parameters are calculated. The ratio of the longitudinal size of LHB can be tuned by altering the relative position of two crystals. As well, the aspect ratio of the LHB is calculated to study the shape of the beam. The LHB array formed by more nonlinear ZnSe crystals is also discussed.

2. Principle description

The schematic setup to generate a LHB is shown in Fig. 1. Two orthogonal incident Gaussian laser beams (GBs) propagate along the x and z direction, respectively. The GB_1 (or GB_2) is collimated by the lenses L_1(or L_2) and then passes through a nonlinear dielectric material ZnSe crystal C_1 (or C_2). Due to the nonlinearity of the ZnSe crystals, the phases of two GBs will be modulated. In each optical path, a hollow beam can be generated after the nonlinear crystal C_1 (or C_2). Two beams are modulated by two crystals, and then superimposed to form a LHB. Such a LHB has a 3D closed hollow region, and the longitudinal size of the hollow beam is much smaller than that generated by a single nonlinear crystal [31].

In theory, the refractive index n of the ZnSe crystal can be described by the relationship

$$n = n_0 + n_2|U|^2 \tag{1}$$

* Corresponding author at: State Key Laboratory of Precise Spectroscopy, School of Physics and Materials Science, East China Normal University, Shanghai 200062, People's Republic of China.
E-mail address: yxia@phy.ecnu.edu.cn (Y. Xia).

https://doi.org/10.1016/j.optcom.2018.03.008
Received 13 November 2017; Received in revised form 30 January 2018; Accepted 5 March 2018
Available online 20 March 2018

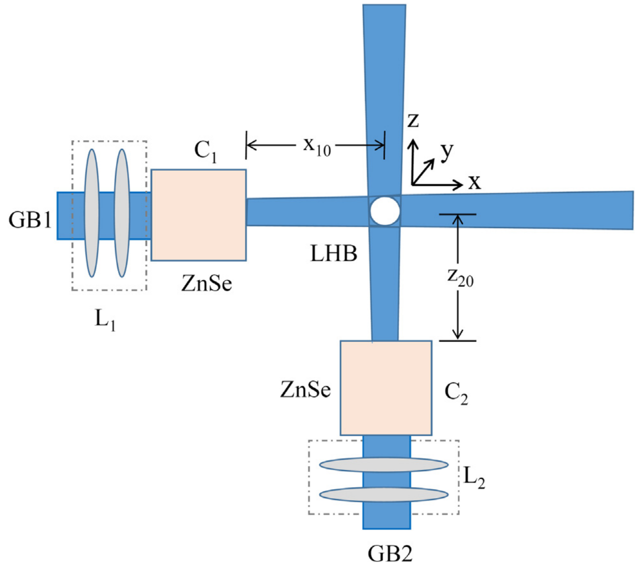

Fig. 1. Schematic diagram to generate a LHB. GB_1 and GB_2 are incident laser beams, L_1 and L_2 are collimated lenses, C_1 and C_2 are nonlinear dielectric material ZnSe crystals, respectively.

Where n_0 and n_2 are the linear and nonlinear refractive indexes, respectively, U is the complex amplitude of the light field.

We set L as the length of the nonlinear ZnSe crystal along the propagating direction and set the center of the superposition of two crossed beams as the coordinate origin. The 2D complex amplitude $U\left(y_1, z_1, -(L+x_{10})\right)$ of the incident well-collimated GB_1 can be described by

$$U\left(y_1, z_1, -(L+x_{10})\right) = U_0\left(y_1, z_1\right) \exp\left(i\varphi_0(y_1, z_1, -(L+x_{10}))\right) \tag{2}$$

where x_{10} is the initial position of the crystal C_1 and $U_0\left(y_1, z_1\right)$ can be expressed as

$$U_0\left(y_1, z_1\right) = U_m \exp\left(-\frac{y_1^2+z_1^2}{w^2}\right) \tag{3}$$

where U_m is the light field complex amplitude, which depends on both the waist radius and power of the incident GB_1. The complex amplitude $U_1(y_1, z_1, -x_{10})$ of the light field at the output face of the nonlinear ZnSe crystal C_1 can be given by

$$\begin{aligned} U_1\left(y_1, z_1, -x_{10}\right) &= U\left(y_1, z_1, -(L+x_{10})\right) \\ &\times \exp\left[i\left(\varphi_0(y_1, z_1, -x_{10}) + n(y_1, z_1)kL\right)\right] \end{aligned} \tag{4}$$

According to the Huygens–Fresnel diffraction theory, the light field complex amplitude $U_1(x, y, z)$ in the propagating position x after the nonlinear ZnSe crystal C_1 can be written as

$$\begin{aligned} U_1(x, y, z) = &\int_{-\infty}^{\infty}\int_{-\infty}^{\infty} \frac{\exp\left(ik\left(x-x_{10}\right)\right)}{i\lambda\left(x-x_{10}\right)} \\ &\exp\left(ik\frac{\left(z-z_1\right)^2+\left(y-y_1\right)^2}{2(x-x_{10})}\right) \\ &U_1\left(y_1, z_1, -x_{10}\right) dy_1 dz_1, \end{aligned} \tag{5}$$

Based on the analysis above, the corresponding light field complex amplitude $U_2(x, y, z)$reshaped by C_2 in the transverse at propagation position z in free space can be written as

$$\begin{aligned} U_2(x, y, z) = &\int_{-\infty}^{\infty}\int_{-\infty}^{\infty} \frac{\exp\left(ik(z-z_{20})\right)}{i\lambda(z-z_{20})} \\ &\exp\left(ik\frac{\left(x-x_2\right)^2+\left(y-y_2\right)^2}{2(z-z_{20})}\right) \\ &U_2\left(x_2, y_2, -z_{20}\right) dx_2 dy_2 \end{aligned} \tag{6}$$

where z_{20} is the initial position of the crystal C_2 and $U_2\left(x_2, y_2, -z_{20}\right)$can be expressed as

$$\begin{aligned} U_2\left(x_2, y_2, -z_{20}\right) = &U\left(x_2, y_2, -(L+z_{20})\right) \exp\left[i\left(\varphi_0\left(x_2, y_2, -z_{20}\right)\right.\right. \\ &\left.\left.+\ n(x_2, y_2)kL\right)\right] \end{aligned} \tag{7}$$

As a result, the intensity $I(x, y, z)$ of the light between two crystals is represented as the superposition of corresponding intensity of light $U_1(x, y, z)$ after crystal C_1 and light $U_2(x, y, z)$ after crystal C_2. It can be written as

$$I(x, y, z) = \left|U_1(x, y, z)\right|^2 + \left|U_2(x, y, z)\right|^2 \tag{8}$$

3. Results and Discussions

To study the propagation characteristics of the LHB in free space, we define the special parameter, the dark spot size (DSS) as the full width at half maximum (FWHM) of the radial-intensity distribution inside the notch of the LHB [3]. Based on the theoretical analyses above, the intensity distributions of the LHB moving the relative position between two nonlinear ZnSe crystals can be calculated by using Eqs. (2)–(8). In the numerical calculation, the waist radius of the two incident GBs is taken as $w_1 = w_2 = 300$ μm, the light field complex amplitude is $U_m = 3.3 \times 10^4 \sqrt{W}/m$ and the wavelength is $\lambda = 447.6$ nm - experimentally from a dye laser. With these light parameters, the significant nonlinear effect of the ZnSe crystal can be excited. For the ZnSe crystal, the length is $L = 450$ μm, n_0 is 2.8 and n_2 is 6.1×10^{-13} m^2/W. According to the calculated results in Ref. [31], an optimal hollow beam can be obtained at a distance $z_{optimal} = 0.62$ m away from the ZnSe crystal under these parameters, the beam is kept to be a ring beam and to be hollow at the beam center for a long distance with ∼0.8 m in the propagating direction, which looks like a hollow ellipsoid with a large elliptical ratio. From our calculation, the intensity distributions of the superposed light beam after crystal C_2 at the different z position and at $x_{10} = x_{optimal} = -0.62$ m are shown in Fig. 2. The left and center columns are the 1D intensity distributions along the x and z direction, respectively, the right column is 2D intensity distributions in xz plane. In Fig. 2, the position of the crystal C_1 is fixed while the position of the crystal C_2 moves along the z direction. The superposed light field appears as a pipe in the z direction where the position of the crystal C_2 is $z_{20} = -0.2$ m (as shown in Fig. 2(m)).

As the position of the crystal C_2 approaches the optimal position $z_{20} = z_{optimal} = -0.62$ m gradually, the light intensity in the x and z direction will have the same hollow profile distributions (as shown in Fig. 2(d), (j)). At the position of the crystal $C_2 z_{20} = x_{10} = -0.62$ m, an optimal 3D closed LHB is formed — it is nearly square (as shown in Fig. 2(p)), and the DSS_z (1.2 mm) of this LHB is much less than DSS_z (0.8 m) that generated by a single ZnSe crystal. So the ratio of the longitudinal size of LHB can be easily changed by altering the relative position of two crystals. The smaller the longitudinal size is, the higher the intensity gradient of the LHB is, so the blue-detuned LHB can be used to trap and cool neutral atoms by intensity-gradient induced Sisyphus cooling. When the position of the crystal C_2 is larger than 0.62 m, the light beam gradually displays a profile with a non-zero central intensity and larger size, and the superposed light beam looks like a pipe in the x direction (as shown in Fig. 2(r)). In this case, the superposed light beam is dominated by the light beam after C_1.

As a result, we study the relationship of the LHB size with the waist radius of the incident GB and the length of the nonlinear ZnSe crystal. Firstly, we assume that two waist radiuses of both GBs are the same, i.e., $w_1 = w_2$. When the positions of the two crystals C_1 and C_2 are fixed at $x_{10} = z_{20} = -0.62$ m, an optimal closed LHB can be obtained. Fig. 3 shows the 2D intensity distributions of the LHBs under the different waist radius of incident GBs. It is evident that all the LHBs are nearly square in xoz plane and the DSS is gradually increasing while increasing the waist radius w. The detailed information about each LHB's size — DSS at x (or z) direction is concluded in Fig. 4. The DSS is linearly related

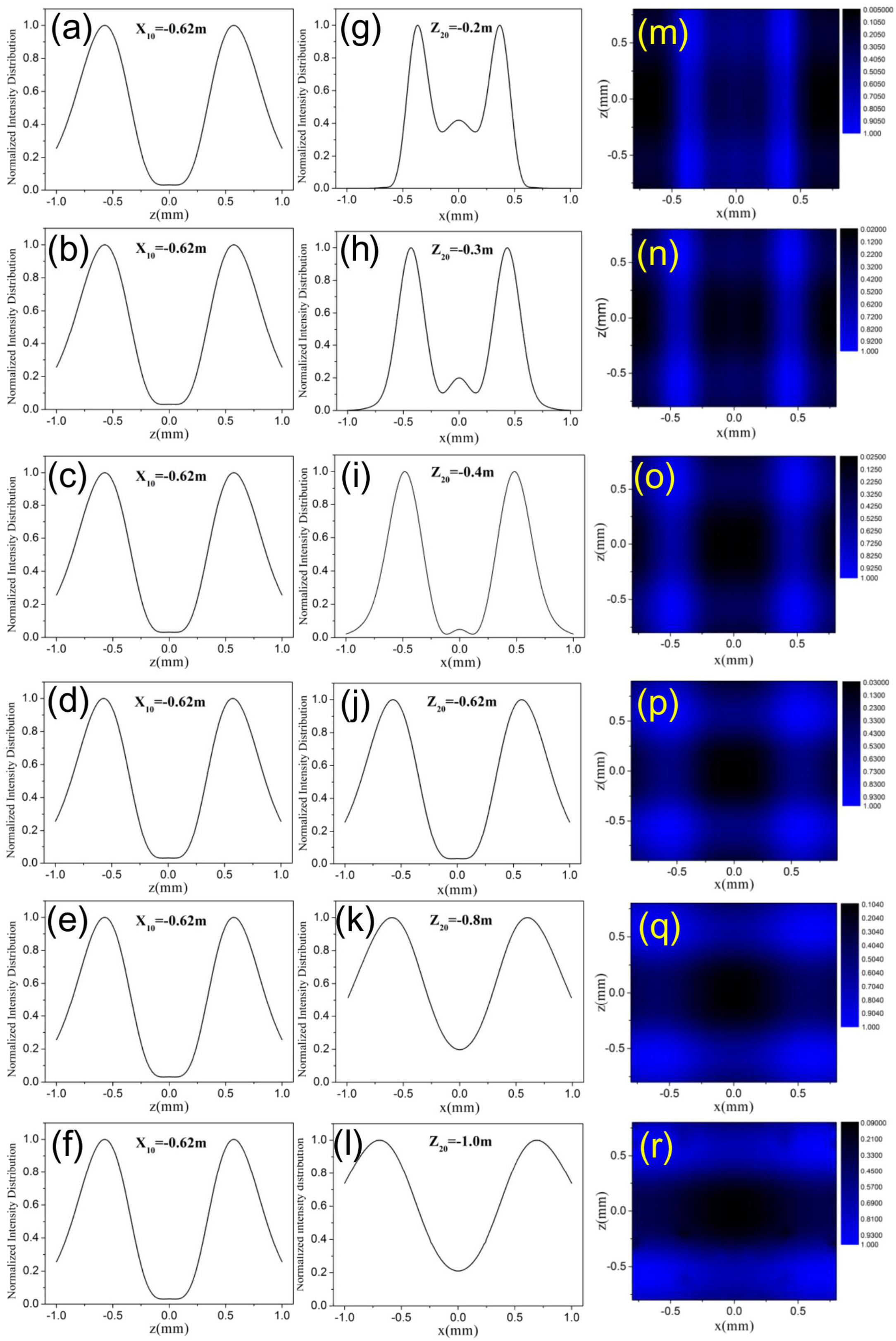

Fig. 2. Calculated and normalized intensity distributions of the superposed beam at various z distances. The left and center columns are the 1D intensity distributions, the right column is 2D intensity distributions in xoz plane.

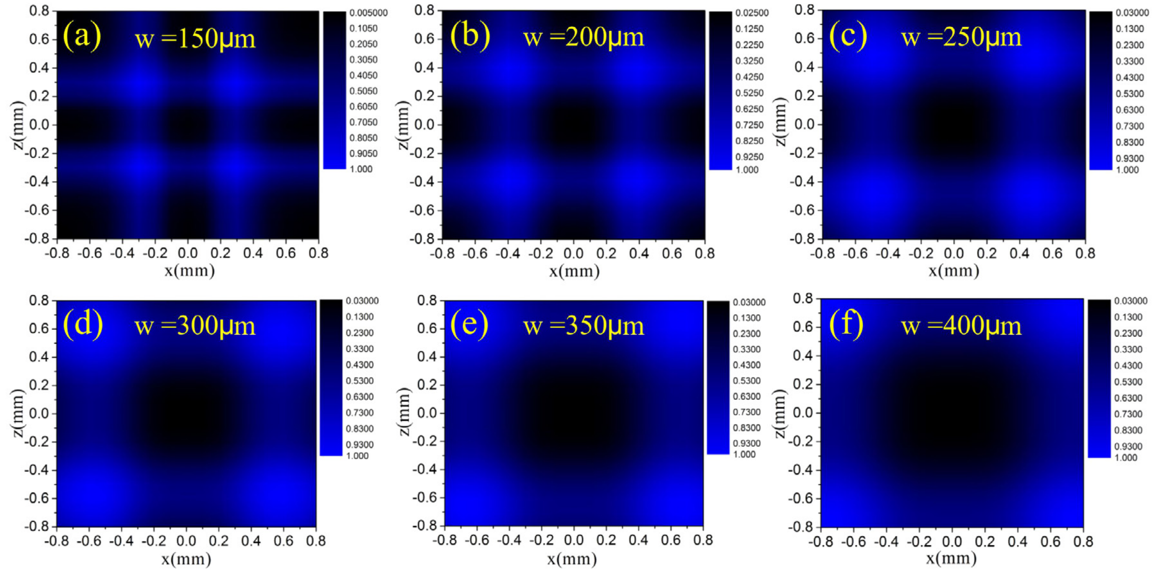

Fig. 3. Calculated and normalized intensity distributions in the case of different waist radius $w = w_1 = w_2$ of incident GBs, the length of each crystal is $L_1 = L_2 = 450$ μm.

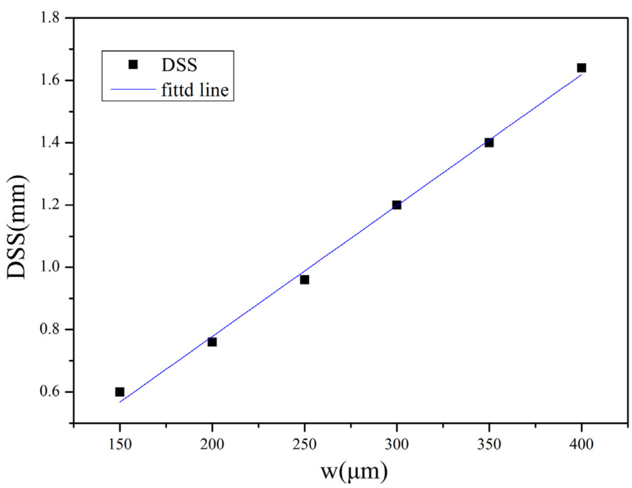

Fig. 4. Dependence of the DSS on the waist radius w of two incident GBs.

to the waist radius w. As the waist radius w is increasing from 150 μm to 400 μm, the LHB size is increasing from 0.6 mm to 1.64 mm.

If the waist radius w_1 and w_2 of the GBs are not the same, the results will be changed. In our numerical simulations, the w_1 is fixed, $w_1 = 300$ μ m. While the w_2 is increasing from 150 μm to 400 μm, the dependence of the 2D intensity distributions of the LHB on the w_2 is shown in Fig. 5. For $w_2 < 300$ μm, a dark hollow beam is formed whose DSS_x is smaller than DSS_z (see Fig. 5(a)–(c)). For $w_2 > 300$ μm, the DSS_x is gradually larger than the DSS_z (see Fig. 5(e) and (f)). In particular, $w_1 = w_2 = 300$ μm, a square dark hollow beam is shown in Fig. 5(d). The relationship between the aspect ratio DSS_x/DSS_z and w_2/w_1 is plotted in Fig. 6. It can be recognized as a linear line.

The principle of the beam-shaping in this scheme is based on the nonlinear interaction between the laser light field and the nonlinear crystal. The interaction situation is also related to the length L of the nonlinear crystal. So we study the influence of the length of ZnSe crystal on the LHB's shape. To simplify, the length L_2 of the crystal C_2 is not changed, $L_2 = 450$ μm, and $w_1 = w_2 = 300$ μm, both the crystals C_1 and C_2 are 0.62 m away from the superposed region. The 2D intensity

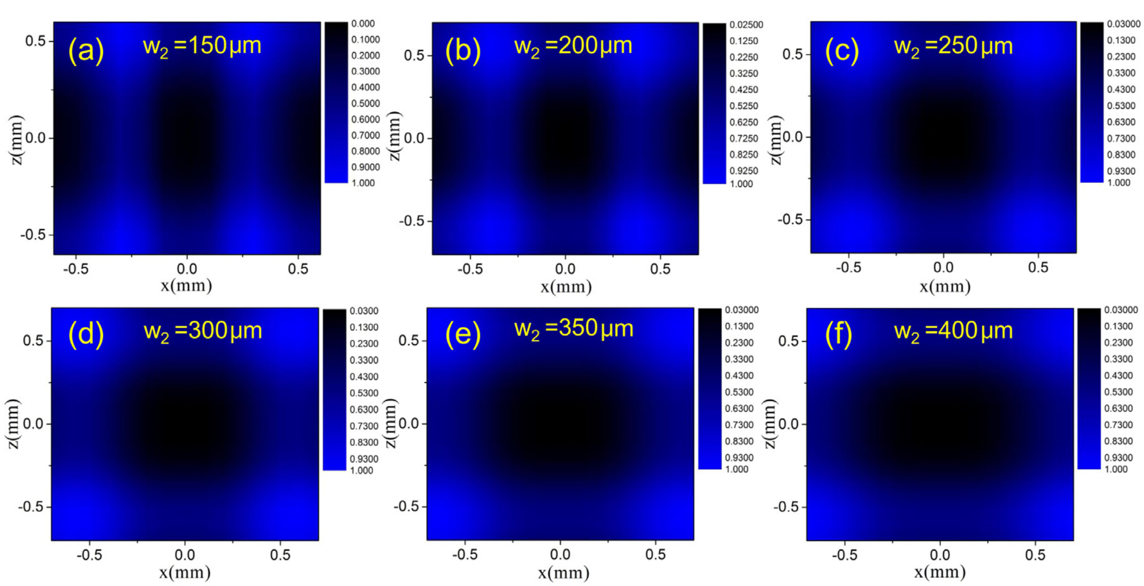

Fig. 5. Calculated and normalized intensity distributions in the incident GBs with the invariable waist ratio $w_1 = 300$ μm and the different waist ratio w_2 at distance $x = z = 0.62$ *m*.

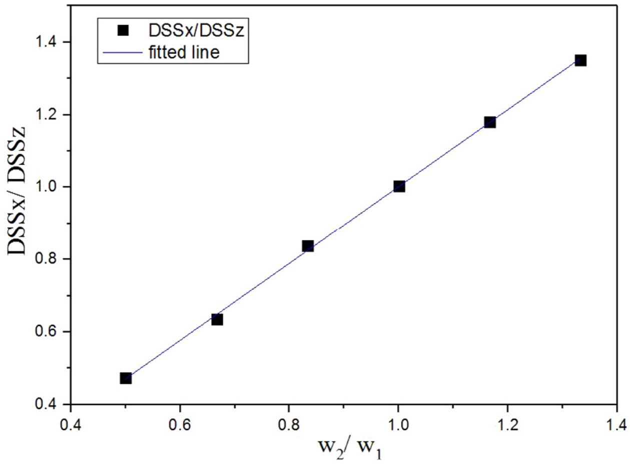

Fig. 6. Dependence of the aspect ratio DSS_x/DSS_z on the waist radius ratio $w_2/w_1, w_1 = 300$ μm.

distributions of the LHBs in the case of different length L_1 of the crystal C_1 are shown in Fig. 7. When the length L_1 is smaller than L_2, the DSS_z of the LHB is smaller than the DSS_x (see Fig. 7(a) and (b)), the aspect ratio DSS_x /DSS_z is >1.0. For $L_1 = L_2 = 450$ μm, as shown in Fig. 7(c), the 2D intensity distribution of the LHB is square. In contrast, a LHB of which DSS_x is smaller than DSS_z is produced for L_1 larger than L_2, as shown in Fig. 7(d)–(f). The relationship between the aspect ratio DSS_x/DSS_z and L_2/L_1 is plotted in Fig. 8. The aspect ratio is increasing with the increasing of the crystal length ratio.

What is more, with the optical system illuminated by four incoherent incident light waves with a cross angle $\pi/2$, a 1D array of the LHB will be formed. The calculated intensity distribution of a 1D LHB array is shown in Fig. 9. In order to obtain the array of the LHB, we choose appropriate length of the crystals as well as the waist radius of the incident GBs. We find that the generated LHB is nearly parallel to each other with a DSS of 2.44 mm when the crystal length is $L = 450$ μm and the waist radius of the incident beam is $w = 1.0$ mm.

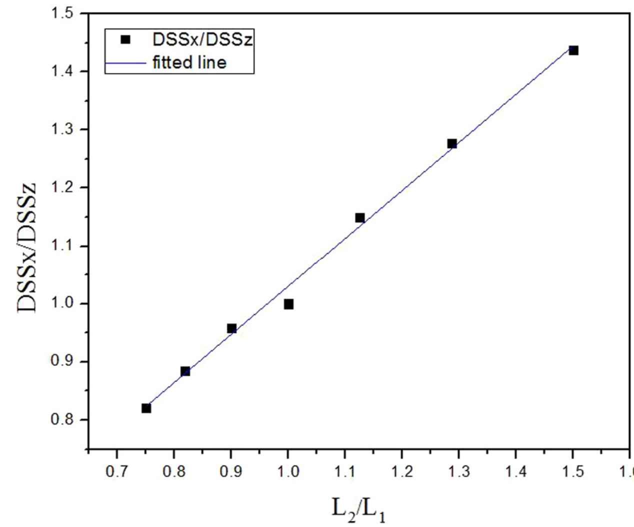

Fig. 8. Dependence of the aspect ratio DSS_x/DSS_z on the length ratio L_2/L_1, $L_2 = 450$ μm.

4. Conclusions

In conclusion, we have proposed a nonlinear optical method to generate a LHB by using crossed nonlinear ZnSe crystals. Our study shows that the longitudinal size of LHB can be changed from 0.8 m to 1.2 mm, which is reduced by ∼ 660 times compared to that generated by a single nonlinear crystal. The dependence of the DSS of LHB on the waist radius of the incident beam, and of the aspect ratio of DSS_x/DSS_z on the waist radius ratio w_2/w_1 and length ratio L_2/L_1 are linear. In addition, the LHB arrays can be formed under the appropriate crystal length and the waist radius of the incident laser beam. Such a LHB has a 3D closed dark hollow region and a large intensity gradient; it can be used to trap cold neutral atoms, molecules and microscopic particles. In particular, the intensity gradient of a LHB may be used to efficiently cool neutral atoms by LHB-induced Sisyphus cooling [7].

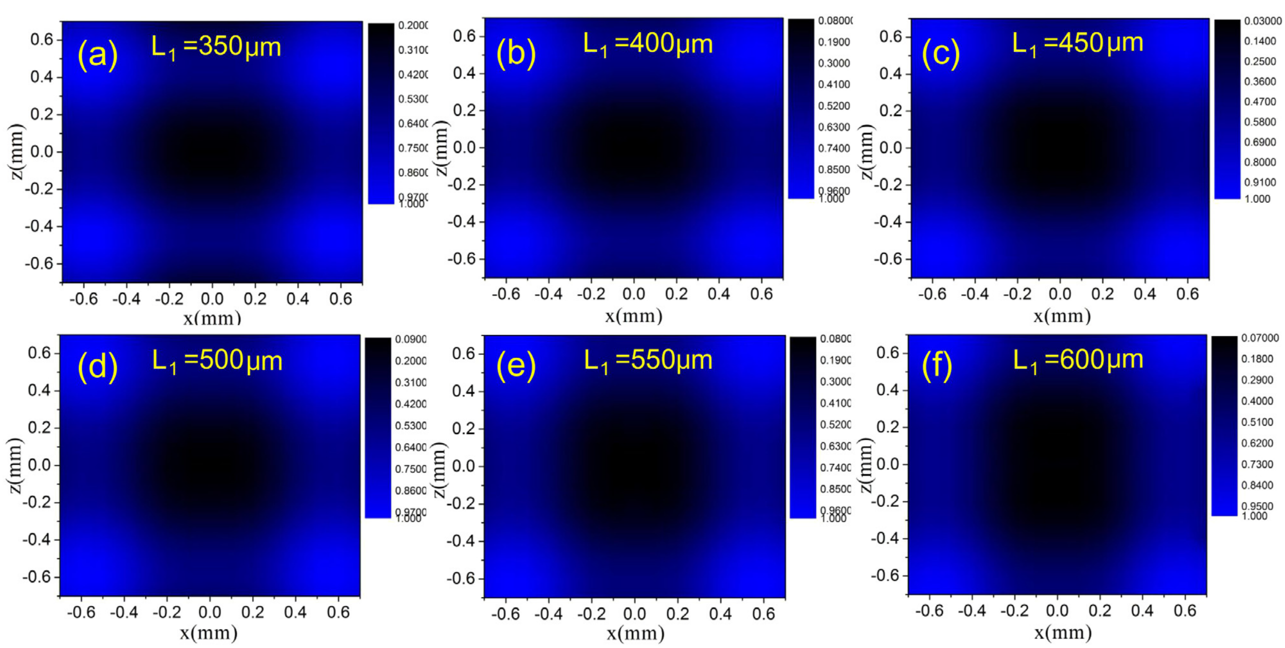

Fig. 7. Calculated and normalized intensity distributions in the case of different length L_1 of ZnSe crystal C_2 for $L_2 = 450$ μm and $w_1 = w_2 = 300$ μm.

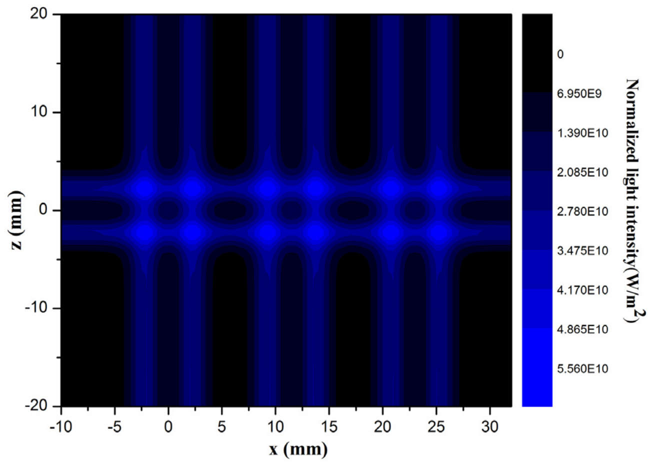

Fig. 9. Intensity distribution of a 1D LHB array.

Acknowledgments

We acknowledge support from the National Natural Science Foundation of China under grants 91536218, 11374100, the Natural Science Foundation of Shanghai Municipality under grant 17ZR1443000.

References

[1] J. Arlt, M.J. Padgett, Generation of a beam with a dark focus surrounded by regions of higher intensity: The optical bottle beam, Opt. Lett. 25 (2000) 191–193.
[2] S. Kulin, S. Aubin, S. Christe, B. Peker, S.L. Rolston, L.A. Orozco, A single hollow-beam optical trap for cold atoms, J. Opt. B 3 (2001) 353–357.
[3] J.P. Yin, W.J. Gao, Y.F. Zhu, Generation of dark hollow beams and their applications, Prog. Opt. 44 (2003) 119–204.
[4] P. Xu, X.D. He, J. Wang, M.S. Zhan, Trapping a single atom in a blue detuned optical bottle beam trap, Opt. Lett. 35 (2010) 2164–2166.
[5] V.G. Shvedov, C. Hnatovsky, A.V. Rode, W. Krolikowski, Robust trapping and manipulation of airborne particles with a bottle beam, Opt. Express 19 (2011) 17350–17356.
[6] S.K. Mondal, S.S. Pal, P. Kapur, Optical fiber nano-tip and 3D bottle beam as non-plasmonic optical tweezers, Opt. Express 20 (2012) 6180–16185.
[7] Y.L. Yin, Y. Xia, R.M. Ren, X.L. Du, J.P. Yin, Intensity-gradient induced sisyphus cooling of a single atom in a localized hollow beam trap, J. Phys. B 48 (2015) 195001–195006.
[8] P. Zhang, Z. Zhang, J. Prakash, S. Huang, D. Hernandez, M. Salazar, D.N. Christodoulides, Z.G. Chen, Trapping and transporting aerosols with a single optical bottle beam generated by moiré techniques, Opt. Lett. 36 (2011) 1491–1493.
[9] L. Cacciapuoti, M.D. Angelis, G. Pierattini, G.M. Tino, Single-beam optical bottle for cold atoms using a conical lens, Eur. Phys. J. D 14 (2001) 373–376.
[10] Y.V. Loiko, A. Turpin, T.K. Kalkandjiev, E.U. Rafailov, J. Mompart, Generating a three-dimensional dark focus from a single conically refracted light beam, Opt. Lett. 38 (2013) 4648–4651.
[11] A. Turpin, V. Shvedov, C. Hnatovsky, Y.V. Loiko, J. Mompart, Optical vault: A reconfigurable bottle beam based on conical refraction of light, Opt. Express 21 (2013) 26335–26340.
[12] T.J. Du, T. Wang, F.T. Wu, Generation of three-dimensional optical bottle beams via focused non-diffracting bessel beam using an axicon, Opt. commun. 317 (2014) 24–28.
[13] V.G. Shvedov, C. Hnatovsky, N. Shostka, W. Krolikowski, Generation of vector bottle beams with a uniaxial crystal, J. Opt. Soc. Am. A 30 (2013) 1–6.
[14] L. Isenhower, W. Williams, A. Dally, M. Saffman, Atom trapping in an interferometrically generated bottle beam trap, Opt. Lett. 34 (2009) 1159–1161.
[15] Y.G. Cheng, J.M. Tong, J.P. Zhu, J.B. Liu, S. Hua, Y. He, Clad photon sieve for generating localized hollow beams, Opt. Laser Eng. 77 (2016) 18–25.
[16] Y.H. Chen, L. Yan, L. Rishøj, P. Steinvurzel, S. Ramachandran, Dynamically tunable optical bottles from an optical fiber, Opt. Lett. 37 (2012) 3327–3329.
[17] H.P. Ye, C. Wan, K. Huang, T.C. Han, J.H. Teng, Y.S. Ping, C.W. Qiu, Creation of vectorial bottle-hollow beam using radially or azimuthally polarized light, Opt. Lett. 39 (2014) 630–633.
[18] G.M. Philip, N.K. Viswanathan, Generation of tunable chain of three-dimensional optical bottle beams via focused multi-ring hollow Gaussian beam, J. Opt. Soc. Am. A 27 (2010) 2394–2401.
[19] P. Genevet, J. Dellinger, R. Blanchard, A. She, M. Petit, B. Cluzel, M.A. Kats, F.D. Fornel, F. Capasso, Generation of two-dimensional plasmonic bottle beams, Opt. Express 21 (2013) 10295–10300.
[20] I. Epstein, A. Arie, Dynamic generation of plasmonic bottle-beams with controlled shape, Opt. Lett. 39 (2014) 3165–3168.
[21] Y. Zhang, X.M. Cheng, X.L. Yin, J.T. Bai, P. Zhao, Z.Y. Ren, Research of far-field diffraction intensity pattern in hot atomic Rb sample, Opt. Express 23 (2015) 5468–5476.
[22] Q. Zhang, X.M. Cheng, H.W. Chen, B. He, Z.Y. Ren, Y. Zhang, J.T. Bai, Diffraction-free self-reconstructing Bessel beam generation using thermal nonlinear optical effect, Appl. Phys. Lett. 111 (2017) 161103.
[23] J.D. Swaim, K.N. David, E.M. Knutson, C. Rios, O. Danaci, R.T. Glasser, Atomic vapor as a source of tunable, non-Gaussian self-reconstructing optical modes, Sci. Rep. 7 (2017) 72411.
[24] S.D. Durbin, S.M. Arakelian, Y.R. Shen, Laser-induced diffraction rings from a nematic-liquid-crystal film, Opt. Lett. 6 (1981) 411–413.
[25] M. Boshier, W. Sandle, Self-focussing in a vapour of two-state atoms, Optics Commun. 42 (1982) 371–376.
[26] Y.R. Shen, Self-focusing: Experimental, Prog. Quantum Electron. 4 (1975) 1–34.
[27] J.H. Marburger, Self-focusing: Theory, Prog. Quantum Electron. 4 (1975) 35–110.
[28] D.N. Christodoulides, M.I. Carvalho, Compression, self-bending, and collapse of Gaussian beams in photorefractive crystals, Opt. Lett. 19 (1994) 1714–1716.
[29] K. Pismennaya, O. Kashin, V. Matusevich, A. Kiessling, R. Kowarschik, Beam self-trapping and self-bending dynamics in a strontium barium niobate crystal, J. Opt. Soc. Amer. B 25 (2008) 136–139.
[30] Y.J. Ding, C.L. Guo, G.A. Swartzlander, J.B. Khurgin, A.E. Kaplan, Spectral measurement of the nonlinear refractive index in ZnSe using self-bending of a pulsed laser beam, Opt. Lett. 15 (1990) 1431–1433.
[31] X.L. Du, Y.L. Yin, G.J. Zheng, C.X. Guo, Y. Sun, Z.N. Zhou, S.J. Bai, H.L. Wang, Y. Xia, J.P. Yin, Generation of a dark hollow beam by a nonlinear ZnSe crystal and its propagation properties in free space: Theoretical analysis, Opt. Commun. 322 (2014) 179–182.